A thermodynamically consistent determination of surface tension of small Lennard-Jones clusters from simulation and theory

Jan Julin,[a] Ismo Napari, Joonas Merikanto, and Hanna Vehkamäki
Department of Physics, University of Helsinki, P.O. Box 64, Helsinki 00014, Finland

(Received 4 March 2010; accepted 2 June 2010; published online 22 July 2010)

We have determined the surface tension of small Lennard-Jones clusters using molecular dynamics and Monte Carlo simulation methods as well as density functional theory calculations. For the two simulation methods the surface tension is calculated via a rigorous thermodynamic route using simulation data as input. The capillary approximation of the classical nucleation theory, where the surface tension of a planar surface is used for cluster surface, is found to be quite reasonable even when the cluster size is as small as 100–150 atoms. For smaller cluster sizes the cluster surface tension is considerably lower than the planar value. We have also obtained an approximative value for the Tolman length by extrapolating to the planar limit the difference between the equimolar radius and the radius of the surface of tension. A negative Tolman length is suggested by all the methods used. © *2010 American Institute of Physics*. [doi:10.1063/1.3456184]

I. INTRODUCTION

Nucleation processes, such as the formation of a liquid cluster from a supersaturated vapor, are highly relevant in many areas of physics. For example, nucleation plays an important role in atmospheric new particle formation.[1] If a molecular cluster that is formed in a supersaturated vapor is to grow to macroscopic sizes, it must first overcome a potential barrier which exists due to the energy cost of creating an interface between the liquid and vapor phases. The cluster on top of this barrier is known as the critical cluster, and its size and formation free energy as well as the rate of appearance of these clusters (nucleation rate) are among the key quantities of nucleation research. Unfortunately the predictions of the usual theoretical description of nucleation, the classical nucleation theory (CNT), are often found to be unsatisfactory. For example, the experimental nucleation rates usually differ from the theoretical prediction by several orders of magnitude.[2]

In CNT several simplifying assumptions are made. One of these assumptions is the capillary approximation: the surface tension of the small cluster is assumed to be that of a macroscopic planar interface. The planar surface tension γ_∞ is used to calculate such quantities as the size of the critical cluster,

$$N^*_{\mathrm{CNT}} = \frac{32\pi\gamma_\infty^3}{3\rho_l^2(\Delta\mu)^3}, \tag{1}$$

and its formation free energy,

$$W^*_{\mathrm{CNT}} = \tfrac{1}{2}N^*_{\mathrm{CNT}}\Delta\mu. \tag{2}$$

Here ρ_l is the bulk liquid density and $\Delta\mu$ is the chemical potential difference between the supersaturated and saturated vapors. The capillary approximation can be reasonable for large clusters, but a cluster consisting of few tens or hundreds of particles has a highly curved surface with properties that may be quite different from the properties of a planar surface. The capillary approximation can be among the reasons behind the discrepancy between theory and experiment.

Expressions for the surface tension and radius of a cluster that is in equilibrium with a surrounding supersaturated vapor can be obtained following the thermodynamic arguments first presented by Gibbs.[3] The treatment results in thermodynamic expressions that do not depend on assumptions of the cluster possessing bulk properties.[3–5] However, these expressions do depend on the choice of the dividing surface between the liquid and vapor phases. The common choice of dividing surface is the surface of tension, a choice that has to be made for the Laplace equation to be valid. The surface tension with respect to the surface of tension is given by[3,4]

$$\gamma_s = \left[\frac{3W^*(\Delta p)^2}{16\pi}\right]^{1/3}, \tag{3}$$

where W^* is the formation free energy of a critical cluster and Δp is the pressure difference between the bulk liquid and vapor phases in chemical equilibrium. The radius of the surface of tension is

$$R_s = \left(\frac{3W^*}{2\pi\Delta p}\right)^{1/3}. \tag{4}$$

In CNT it is further assumed that the surface of tension coincides with the equimolar surface, the radius of which is given by

$$R_e = \left(\frac{3N^*}{4\pi\Delta\rho}\right)^{1/3}, \tag{5}$$

where N^* is the size of a critical cluster and $\Delta\rho$ is the density difference between bulk liquid and vapor phases in chemical equilibrium.

[a]Electronic mail: jan.julin@helsinki.fi.

If the cluster size is very large the dependence of surface tension on cluster size can be expressed using Tolman's equation,[6]

$$\frac{\gamma_s}{\gamma_\infty} = \frac{R_s}{R_s + 2\delta_\infty}, \tag{6}$$

where δ_∞ is the Tolman length, defined as the difference between the radius of the equimolar surface and the radius of the surface of tension at the planar limit. Equation (6) becomes valid at cluster sizes larger than 10^6 atoms,[4] and is thus inapplicable to the relatively small nucleating clusters. However, the Tolman length is important as a first correction to the surface tension, and its sign sheds light on the behavior of surface tension as a function of cluster size.

Determining the surface tension of the nanometer-scale nucleating clusters experimentally is impossible, but various computational and theoretical methods can be employed to gain insight on the cluster surface tension. Such methods include molecular dynamics (MD) simulations,[7–9] Monte Carlo (MC) simulations,[10,11] and density functional theory (DFT) calculations.[4,12–14] There are several ways to obtain cluster surface tension from simulations, for example, one can use the mechanical description of surface tension calculated with the aid of the pressure tensor. However, the mechanical surface tension does not equal the thermodynamic surface tension, the location of the surface of tension in these two descriptions differs, and the mechanical route may even lead to unphysical results.[10] Alternatively, certain approximative thermodynamic routes exist, but they are only exact in the limit of large clusters.[7,15]

In this work we utilize the rigorous thermodynamic expression, Eq. (3), using MD and MC simulation results on critical sizes and formation free energies of Lennard-Jones clusters from our earlier work[16] as input. The bulk pressures and densities for the two phases are obtained by MD simulations. The cluster sizes studied are in the 20–300 size range for MD and 20–500 for MC. The resulting MD and MC surface tensions are compared with DFT results.

This paper is organized as follows. Simulation details are described in Sec. II. In Sec. III, results on surface tension and the dividing surface radii, as well as predictions on Tolman length, are presented and discussed. Conclusions are summarized in Sec. IV.

II. METHODS

The cluster formation free energies and critical sizes were simulated in our earlier work,[16] where a more detailed description of the simulation methods can be found. The work included MD and MC simulations along with DFT calculations of Lennard-Jones argon with the potential cut and shifted at 5σ, where σ is the Lennard-Jones length parameter. All simulations were performed at a reduced temperature of $T=0.662$, which should be close to the triple point of the potential model.[16] In this section the key simulation details are summarized.

A. MD simulations

The formation free energy of the critical cluster is a quantity that can be relatively easily obtained from both MC and DFT for a wide range of cluster sizes. Formation free energies can also be obtained as a simulation result from MD when using the direct nucleation simulation method,[9,17] in which a supersaturated vapor is simulated until a nucleation event is observed. However, computational limitations restrict achievable critical cluster sizes in direct simulations usually to few tens of atoms. This is due to the fact that the lower the supersaturation, the longer on average the simulation must be run until nucleation onset occurs. To study larger critical clusters with MD, the alternative approach of the so-called indirect nucleation simulations is sometimes employed.[9,18] In the indirect method, a pre-existing cluster in equilibrium with surrounding vapor is simulated and simulation results include the critical size and vapor properties. However, formation free energy is not obtained from the simulations as the cluster exists already at the beginning of the simulation.

In Ref. 16 we performed both direct and indirect MD simulations, and using the nucleation theorem,

$$\frac{\partial W^*}{\partial \Delta\mu} = -N^*, \tag{7}$$

we calculated formation free energies also for the clusters in the indirect simulations. With ten different cluster sizes obtained from indirect simulations and one size from direct simulations, the critical sizes were plotted as a function of $(\Delta\mu)^{-3}$. As in CNT [Eq. (1)], the resulting dependence was linear, although with a slope different from the CNT prediction, and the direct simulation point was located on the same line as the indirect simulation points. Using a linear fit made to the $N^*(\Delta\mu^{-3})$ plot, we then integrated the nucleation theorem, Eq. (7), with the direct simulation formation free energy acting as a reference point. The resulting formation free energies are used in the calculations of the present work.

In addition to the formation free energies, we need the pressure difference of the bulk phases to calculate the surface tension using Eq. (3). To calculate the pressure-density correlations for the two phases, we performed MD simulations of bulk liquid and vapor at various densities. For the metastable vapor we used the method of Linhart *et al.*,[19] and we used the pressure-density correlation simulated by us in Ref. 16. The simulations were performed at several densities up to $\rho_v' = 0.025$ and the system consisted of 1000 atoms. Obtaining the liquid pressure-density correlation is even more straightforward, as the liquid is not deeply in a metastable state. We simulated a system of 1728 atoms at several liquid densities ranging from $\rho_l = 0.84$ to $\rho_l = 0.93$. For both vapor and liquid, the simulated points were fitted to a sixth-order polynomial function, resulting in an expression for $p(\rho)$. The chemical potential as a function of density was then obtained by integration using the Gibbs–Duhem equation. As the vapor density of the simulations is a known quantity, the vapor pressure and the vapor chemical potential can then be calculated. The fact that the two phases are in chemical equilibrium is

used to find the corresponding liquid pressure: equating the chemical potentials of the two phases reveals the liquid density, and consequently the liquid pressure.

For consistency, the pressure-density correlations obtained with MD are used also to calculate the MC cluster surface tensions.

In addition to these simulations, MD simulations of a planar liquid-vapor interface were performed in Ref. 16 to determine the equilibrium vapor density, the bulk liquid density, and the surface tension of a planar interface.

B. MC simulations

The MC method used in Ref. 16 is the growth-decay method of Merikanto *et al.* which is described in detail in Refs. 20 and 21. The simulated system consisted of a single cluster, which was defined according to the Stillinger criterion.[22] No new MC simulations were performed for the present work, but unlike Ref. 16 where the MC formation free energies and critical sizes were presented only for the supersaturations corresponding the MD simulated clusters, we have now calculated these quantities for considerably higher number of different supersaturations from the existing MC data. This kind of calculation is made possible by the fact that the growth-decay MC formation free energy of a cluster of size N can be written as[23]

$$W_{N,\mathrm{MC}} = -k_B T \sum_{N'=2}^{N} \ln\left[\frac{\bar{G}_{N'-1}(T,S=1)}{\bar{D}_{N'}(T,S=1)}\right] - k_B T(N-1)\ln S, \tag{8}$$

where $\bar{G}_N$ and $\bar{D}_N$ are the grand canonical growth and decay rates, respectively, and S is the saturation ratio. From Eq. (8) it is clear that knowing the formation free energy in one supersaturation allows the calculation of W in another supersaturation. As long as the critical size of the new supersaturation is among the sizes one has the data for, it can be recognized from the maximum value of W.

The results of Ref. 16 showed that the critical sizes from MD and DFT agreed well, but the MC critical sizes were smaller than the others. The same was true for formation free energies, although the MD and DFT formation free energies did not agree quite as well as the critical sizes did. However, the MC values for the equilibrium vapor density and planar surface tension, which were calculated with the aid of the MD bulk liquid density, were in very good agreement with MD. The planar surface tension obtained from MD was $\gamma_\infty = 1.107$ (given in the reduced Lennard-Jones units) and the MC value was $\gamma_\infty = 1.115$.

C. DFT calculations

The DFT approach used in the present work is the so-called perturbative DFT.[24] To allow a meaningful comparison between DFT and simulation, the Lennard–Jones parameters and the hard-sphere diameter were fitted to reproduce the MD bulk equilibrium values (equilibrium vapor pressure, bulk liquid density, planar surface tension) that were obtained from the planar interface simulations.[16,25] In our previous study the DFT calculations were performed only for the vapor conditions of the MD simulations. In this study the DFT calculations were extended to conditions corresponding to cluster sizes of the order of 10^6 atoms, which is considerably larger than the cluster sizes of the simulations.

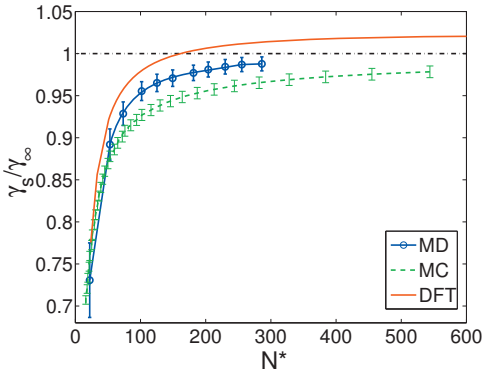

FIG. 1. Cluster surface tension divided by surface tension of a planar interface plotted as a function of cluster size. The circles denote the sizes observed in the MD simulations.

III. RESULTS AND DISCUSSION

The cluster surface tensions obtained with Eq. (3) are plotted as a function of the cluster size in Fig. 1. The cluster surface tensions are divided by the surface tension of the planar interface γ_∞. When plotting the MD and MC points, we have used their respective values for planar surface tension from Ref. 16. The DFT points use the MD value of γ_∞ as the DFT parameters were fitted to reproduce the MD bulk properties. The circles denote the cluster sizes of the MD simulations, with the smallest size corresponding to the direct simulations and the rest to the indirect ones. The smallest MC cluster for which the surface tension is plotted contains 15 atoms. While MC formation free energies were available even for dimers, smaller critical sizes than 15 would have corresponded to supersaturations so high that our simulated pressure-density correlation would have been no longer valid. The uncertainties for MD and MC are caused by the uncertainty in the planar surface tension and the uncertainty in the formation free energies.

Figure 1 suggests that the capillary approximation is quite reasonable even when the cluster has as few as 100–150 atoms. While there is some disagreement between the different methods, all of them are within 5% of the planar value already when the cluster size exceeds 150 atoms. For all the methods the cluster surface tension for clusters smaller than 100 atoms is smaller than the planar value; this is the size range of the critical clusters found in the conditions of typical nucleation experiments.

The considerable difference between the MD and MC cluster surface tensions as seen in Fig. 1 cannot be explained by the difference in the value used for the planar surface tension γ_∞, as the MD and MC values for planar surface tension are so close to each other. The MD and MC surface tensions are calculated according to Eq. (3) and the same pressure-density correlation is used for both of them, so the main reason behind the difference between MD and MC sur-

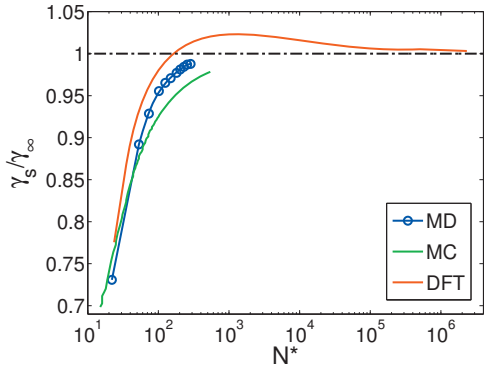

FIG. 2. DFT surface tension for a larger cluster size range, showing that the DFT values approach the planar value when cluster size becomes large. The MD and MC points from Fig. 1 are also plotted. The error bars have been omitted for clarity.

face tensions is the difference in the formation free energies between the two methods. Since also the MD and MC critical sizes were different in the same vapor conditions,[16] the difference between the cluster surface tensions in Fig. 1 is also necessarily affected by the fact that they are plotted as a function of critical size. However, this difference in critical size has only a very minor effect on the surface tension difference seen in Fig. 1. The MD and DFT cluster surface tensions do not exhibit the relatively good agreement that was seen between the critical sizes and formation free energies from these two methods.

The DFT cluster surface tensions actually exceed the planar value for clusters larger than about 150 atoms. This kind of behavior has been found also in earlier DFT studies,[4,14] and at larger sizes these studies found the cluster surface tension approaching the planar value again. This is true also for the present DFT results, as is seen in Fig. 2 where the surface tension is plotted for a wider range of cluster sizes.

In Fig. 3 the difference between the equimolar radius and the radius of the surface of tension is plotted as a function of $\Delta\mu$, the chemical potential difference between supersaturated and saturated vapors. Reduced Lennard-Jones units

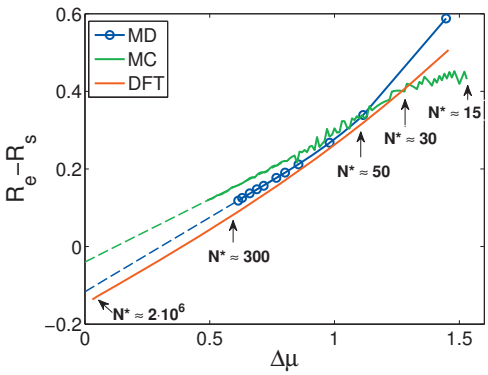

FIG. 3. The difference between the equimolar radius and the radius of surface of tension as a function of chemical potential difference. The dashed lines are extrapolations from the MD and MC data using the linear dependence seen for the larger clusters. The circles denote the $\Delta\mu$ of the MD simulations. $\Delta\mu=0$ corresponds to the planar limit. To give a general idea how different values of $\Delta\mu$ relate to the critical cluster size, some example sizes are shown in the figure.

are used in the figure. The circles represent again the points corresponding to the supersaturations of the MD simulations, and the point corresponding to the direct simulations is now the one with largest $\Delta\mu$. To give a general idea how $\Delta\mu$ relates to the critical size, some example sizes are shown in the Fig. 3. It should be noted that these are approximate values, and the critical size corresponding to a given value of $\Delta\mu$ differs between the methods.

When $\Delta\mu \lesssim 1$ the different methods exhibit qualitatively similar behavior: linear scaling with $\Delta\mu$. In particular, all of the methods would seem to predict a negative Tolman length (which is the value of R_e-R_s at the limit $\Delta\mu=0$). Although in Fig. 3 only the DFT results span to cluster sizes where the difference R_e-R_s takes negative values, there seems to be no reason to expect deviation from the linear trend seen for the larger MD and MC clusters as $\Delta\mu \to 0$. Extrapolation of this linear dependence is plotted for MC and MD in Fig. 3 with dashed lines. The predicted Tolman lengths are $\delta_\infty \approx -0.04 \pm 0.02$ from MC, $\delta_\infty \approx -0.12 \pm 0.02$ from MD, and $\delta_\infty \approx -0.15$ from DFT. The uncertainty in MD and MC is estimated from uncertainties in the formation free energies and critical sizes.

While the qualitative behavior of the different methods in Fig. 3 is similar for lower supersaturations (low $\Delta\mu$), there exists a peculiar difference for high supersaturations. For MC the linear slope seen for low supersaturations changes noticeably at higher supersaturations. The change occurs when the cluster size is approximately 30 atoms. For MD and especially DFT there is not an equally noticeable change and unlike MC, where the slope becomes smaller at higher supersaturations, the MD and DFT slopes increase slightly as $\Delta\mu$ grows.

The MC simulations do not take into account interactions between the cluster and surrounding vapor, an assumption that is valid at lower vapor densities where the vapor can be considered to behave as an ideal gas. However, as the simulated pressure-density correlation of the vapor phase reveals,[16] the vapor is quite nonideal at the larger values of $\Delta\mu$ considered here. While the vapor is practically ideal when $\Delta\mu \lesssim 0.85$, the vapor pressure is about 87% of the ideal gas pressure when the MC and DFT plots intersect, and only about 75% at densities corresponding to the largest $\Delta\mu$ values in Fig. 3. The contributions to the critical cluster formation free energy due to cluster-vapor interactions can be of the order of few k_BT,[26] and this could possibly explain why the MC slope behaves differently compared to the other methods at large $\Delta\mu$ in Fig. 3.

A negative Tolman length is commonly predicted by DFT,[13,27,28] but determining the Tolman length from simulations of a planar vapor-liquid interface has resulted in a small but positive value.[10,29,30] However, recently van Giessen and Blokhuis[28] found a negative Tolman length using MD cluster simulations. The negative Tolman length was found by extrapolating cluster simulation data to the planar limit, with the aid of the Laplace equation written in terms of R_e. The values for Δp and R_e were obtained from cluster simulations. Also, they determined the Tolman length from simulations of a planar interface and found a positive value as usual. Interestingly, the predicted negative MD and MC Tolman lengths

of the present work are also determined as an extrapolation from cluster data, although in a different manner than in Ref. 28. Furthermore, both extrapolations yield a MD Tolman length that is closer to zero than the DFT one. The values of the MD Tolman length of the present work (-0.12 ± 0.02) and Ref. 28 (-0.10 ± 0.02) are also quite close to each other, but as the temperature and potential cutoff are different this may be purely coincidental. The reason behind the difference in the sign of δ_∞ when using either planar interface simulations or cluster simulations remains unclear. Some possible causes are discussed in Ref. 28.

Since Tolman's equation [Eq. (6)] works for large cluster sizes,[4,6] a negative Tolman length implies that the surface tension of a large cluster would be greater than the planar surface tension. Negative MD and MC Tolman lengths would thus mean that at some cluster size beyond the size range studied here, also the MD and MC cluster surface tension should exceed the planar value and exhibit similar behavior as the DFT values in Fig. 2.

Very recently a negative Tolman length was also predicted from MD cluster simulations by Sampayo *et al.*,[31] although with a reported uncertainty that does not exclude a positive value.

When using the nucleation theorem in the fashion described in Sec. II A to obtain the MD formation free energies for larger critical clusters, it is assumed that the clusters in the stable equilibrium of the indirect simulations do not differ from the critical clusters of the same size in "unstable equilibrium" at the top of the potential barrier. This is a common assumption, and one that is integral to the idea that indirect simulations can be used to describe critical clusters. However, we have recently reported results that show that the properties of equilibrium clusters and critical clusters may not always be the same.[32] Reference 32 contains both direct and indirect simulations at same vapor conditions and reveals that the structure of the critical cluster is more fragmented than that of the equilibrium cluster of the indirect simulation. However, the difference becomes smaller as temperature decreases. As the temperature in this paper and in Ref. 16 is close to the triple point, it is reasonable to expect that the critical cluster does not have a very fragmented structure and so the equilibrium cluster would be a reasonable approximation of the critical cluster.

IV. CONCLUSIONS

We have studied the surface tension of Lennard-Jones clusters using MD, MC, and DFT methods. The MD and MC surface tensions were calculated using an expression that follows from a rigorous thermodynamic treatment of a cluster-vapor system. The capillary approximation, where the surface tension of clusters is assumed to be equal to that of a planar interface, was found to be a relatively good assumption for clusters larger than about 150 atoms, as the cluster surface tensions for these clusters were within 5% of the planar value. For clusters smaller than 100 atoms all methods predict the cluster surface tension to be lower than the planar surface tension. For these clusters the surface tension increases rapidly with growing cluster size. For DFT it was found that the cluster surface tension exceeded the planar value at relatively small cluster sizes. This behavior is in accordance with previously reported DFT results.

We also calculated the difference between the radius of the equimolar surface and the radius of the surface of tension for the clusters. As the Tolman length is defined as the difference of these radii at the planar limit, an estimate for it can be found by extrapolating the cluster data. Such extrapolation indicates a negative Tolman length for all the methods considered. While commonly predicted by DFT,[13,27,28] a negative Tolman length is not found when simulating a planar liquid-vapor interface.[10,29,30] However, extrapolation from cluster data, with a different method than the one used here, has also earlier pointed to a negative Tolman length.[28] Why cluster simulations would indicate a different sign for Tolman length than planar interface simulations is a question that certainly merits further investigation.

ACKNOWLEDGMENTS

This research was supported by the Academy of Finland Center of Excellence program (Project No. 1118615). The authors would like to thank Dr. Matthew J. McGrath for fruitful discussions.

[1] M. Kulmala, H. Vehkamäki, T. Petäjä, M. Dal Maso, A. Lauri, V.-M. Kerminen, W. Birmili, and P. H. McMurry, J. Aerosol Sci. **35**, 143 (2004).
[2] V. I. Kalikmanov, J. Wölk, and T. Kraska, J. Chem. Phys. **128**, 124506 (2008).
[3] J. W. Gibbs, *Scientific Papers* (Longmans Green, London, 1906), Vol. 1.
[4] K. Koga, X. C. Zeng, and K. A. Shchekin, J. Chem. Phys. **109**, 4063 (1998).
[5] H. Vehkamäki, *Classical Nucleation Theory in Multicomponent Systems* (Springer, Berlin, Heidelberg, 2006).
[6] R. C. Tolman, J. Chem. Phys. **17**, 333 (1949).
[7] M. J. P. Nijmeijer, C. Bruin, A. B. van Woerkom, A. F. Bakker, and J. M. J. van Leeuwen, J. Chem. Phys. **96**, 565 (1992).
[8] J. Vrabec, G. K. Kedia, G. Fuchs, and H. Hasse, Mol. Phys. **104**, 1509 (2006).
[9] M. Horsch, J. Vrabec, and H. Hasse, Phys. Rev. E **78**, 011603 (2008).
[10] P. R. ten Wolde and D. Frenkel, J. Chem. Phys. **109**, 9901 (1998).
[11] M. Schrader, P. Virnau, and K. Binder, Phys. Rev. E **79**, 061104 (2009).
[12] T. V. Bykov and A. K. Shchekin, Colloid J. **61**, 144 (1999).
[13] J. C. Barrett, J. Chem. Phys. **124**, 144705 (2006).
[14] I. Napari and A. Laaksonen, J. Chem. Phys. **126**, 134503 (2007).
[15] S. M. Thompson, K. E. Gubbins, J. P. R. B. Walton, R. A. R. Chantry, and J. S. Rowlinson, J. Chem. Phys. **81**, 530 (1984).
[16] J. Julin, I. Napari, J. Merikanto, and H. Vehkamäki, J. Chem. Phys. **129**, 234506 (2008).
[17] J. Wedekind, R. Strey, and D. Reguera, J. Chem. Phys. **126**, 134103 (2007).
[18] K. Laasonen, S. Wonczak, R. Strey, and A. Laaksonen, J. Chem. Phys. **113**, 9741 (2000).
[19] A. Linhart, C.-C. Chen, J. Vrabec, and H. Hasse, J. Chem. Phys. **122**, 144506 (2005).
[20] J. Merikanto, H. Vehkamäki, and E. Zapadinsky, J. Chem. Phys. **121**, 914 (2004).
[21] A. Lauri, J. Merikanto, E. Zapadinsky, and H. Vehkamäki, Atmos. Res. **82**, 489 (2006).
[22] F. H. Stillinger, J. Chem. Phys. **38**, 1486 (1963).
[23] J. Merikanto, E. Zapadinsky, A. Lauri, and H. Vehkamäki, Phys. Rev. Lett. **98**, 145702 (2007).
[24] X. C. Zeng and D. W. Oxtoby, J. Chem. Phys. **94**, 4472 (1991).
[25] R. M. Nyquist, V. Talanquer, and D. W. Oxtoby, J. Chem. Phys. **103**, 1175 (1995).
[26] K. J. Oh and C. Zeng X, J. Chem. Phys. **112**, 294 (2000).

[27] V. Talanquer and D. W. Oxtoby, J. Phys. Chem. **99**, 2865 (1995).
[28] A. E. van Giessen and E. M. Blokhuis, J. Chem. Phys. **131**, 164705 (2009).
[29] Y. A. Lei, T. Bykov, S. Yoo, and X. C. Zeng, J. Am. Chem. Soc. **127**, 15346 (2005).
[30] A. E. van Giessen and E. M. Blokhuis, J. Chem. Phys. **116**, 302 (2002).
[31] J. G. Sampayo, A. Malijevský, E. A. Müller, E. de Miguel, and G. Jackson, J. Chem. Phys. **132**, 141101 (2010).
[32] I. Napari, J. Julin, and H. Vehkamäki, J. Chem. Phys. **131**, 244511 (2009).